Actin filaments as the fast pathways for calcium ions involved in auditory processes

MILJKO V SATARIC, DALIBOR L SEKULIC* and BOGDAN M SATARIC
Faculty of Technical Sciences, University of Novi Sad, Trg Dositeja Obradovića 6, 21000, Novi Sad, Serbia

**Corresponding author (Email, dalsek@uns.ac.rs)*

We investigated the polyelectrolyte properties of actin filaments which are in interaction with myosin motors, basic participants in mechano-electrical transduction in the stereocilia of the inner ear. Here, we elaborated a model in which actin filaments play the role of guides or pathways for localized flow of calcium ions. It is well recognized that calcium ions are implicated in tuning of actin-myosin cross-bridge interaction, which controls the mechanical property of hair bundle. Actin filaments enable much more efficient delivery of calcium ions and faster mechanism for their distribution within the stereocilia. With this model we were able to semiquantitatively explain experimental evidences regarding the way of how calcium ions tune the mechanosensitivity of hair cells.

[Sataric MV, Sekulic DL and Sataric BM 2015 Actin filaments as the fast pathways for calcium ions involved in auditory processes. *J. Biosci.* **40** 549–559] DOI 10.1007/s12038-015-9547-z

1. Introduction

Hair cells are mechanosensitive receptors of vertebrate inner ears that are specialized to transform mechanical motion into the change in membrane potential and to initiate the pertaining ionic currents. Each hair cell is equipped with the hair bundles which comprise the hexagonal arrays of so called stereocilia. Every stereocilium is a bundle of parallel actin filaments interconnected with different lateral links. The tip links are especially important since they serve for opening and closing of ionic channels in cell membrane. The hair bundle is arranged like a harp or the back acoustic compartment of a piano in rows of increasing height (Helmholtz 1954), see figure 1. As an example, in striolar hair bundle from chicks the tallest stereocilia are 9.2 μm height and the shortest are 2.4 μm. The number of stereocilia in that bundle is 51. Diameter of a single stereocilium is 0.4 μm and the number of tip links in this bundle is 42.

When the hair bundle is pushed in positive (right) direction (figure 2A), the spring of tip-link exerts a force on the trap door and thus opens the ionic channel. It enables the influx of positive K^+ and Ca^{2+} ions inside stereocilia endolymph. Deflecting the hair bundle in the opposite direction, the tip-link is getting compressed, thus closing the trap door of channel and preventing the ionic influx (figure 2B) (Nam *et al*. 2006). The number of open channels depends largely on the deflecting position of the bundle and not on its velocity or acceleration of movement. But, opening dynamics should depend on frequency of movement thus enabling the essential selectivity of hair cells.

It is widely recognized that mechano-electrical transduction in hair bundles posits that force-generating myosin motors regulate the elastic properties of the transduction channels as being tuned by the concentration of Ca^{2+} ions. Namely, the cross-bridge cycle of Myo1c motor protein is calcium sensitive (Gillespie and Cyr 2004; Adamek *et al*. 2008). Myosin motors Myo1c are responsible for anchoring the channel's mechanical complex to the actin filament core of the stereocilia forming the cross-bridge. In the relaxed state troponin molecule forms a tropomyosin complex which blocks the attachment site for the actin-myosin cross-bridge. The Ca^{2+} ion attaches to troponin, causing it to change shape thus exposing the binding site for myosin on the actin filament. Such troponin role in stereocilia is widely elaborated by Karkanevatos (2001). Since the channel is permeable to Ca^{2+} ions, its opening tunes the local intrabundle

Keywords. Actin filament; calcium ions; hair cell; polyelectrolyte; stereocilia

Published online: 14 August 2015

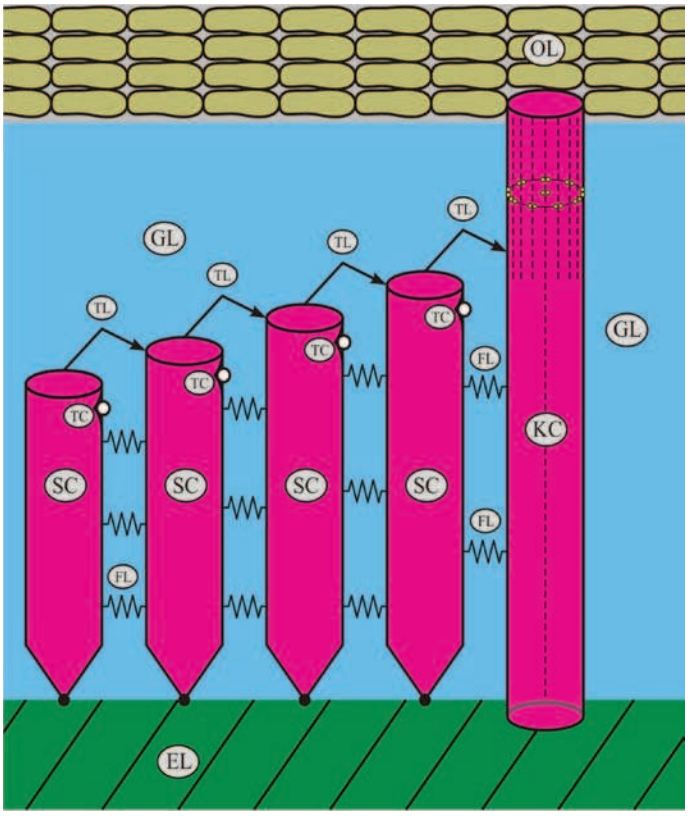

Figure 1. The sketch of single row of stereocilia (SC) within a hair bundle of vestibular hair cell. The row of stereocilia (SC) is interconnected by filamentous links (FL) and finished with a single kinocilium (KC). The tip links (TL) and pertaining transduction channels (TC) are responsible for ionic currents. Epithelial layer (EL), otholitic layer (OL) and gelatinous layer (GL) are also depicted.

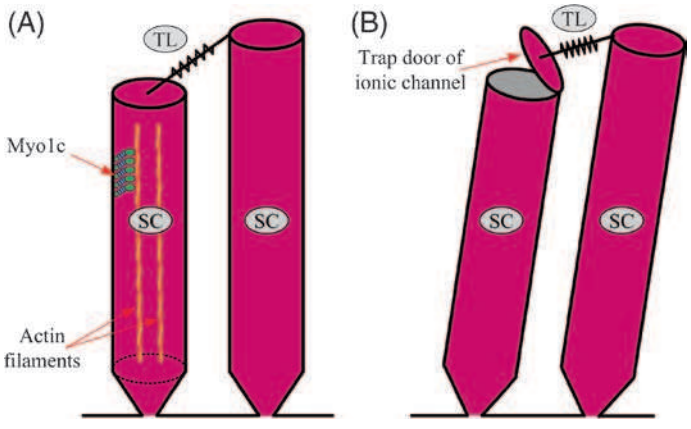

Figure 2. A model of mechano-electrical transduction in hair bundles. (**A**) Schematic illustration of two adjacent stereocilia (SC) with tip-link (TL) joining two ion channels and Myo1c motors in interaction with actin filaments. (**B**) Hair bundle is deflected with a positive stimulus; spring of tip-link exerts a force on the trap door and opens the ionic channel.

Ca^{2+} concentration which in turn regulates the force generated by Myo1c motors and it is manifested through channel reclosure.

There is a sharp but essentially nonlinear mechanical tuning of auditory process within the hair cells with oscillating bundles. Although the bundle's response far from the resonance's center is linear, at the resonance peak the response increases sublinearly, actually logarithmically, compressing almost 80 dB into about 20 dB (Ruggero 1992). It is apparent that auditory sensitivity is developed by an active amplificatory process whose exact nature still remains to be completely explained.

It is the prevailing view that Myo1c motors propel these active oscillations of hair bundles as being powered by the energy supply provided by ATP hydrolysis. Calcium obviously affects the probability of a Myo1c motor to be bound to actin, and more than that, it impacts the stiffness of an actin-myosin cross-bridge controlling the amount of the power stroke of a single motor (Martin *et al*. 2003).

It was shown that the time course of channel activation and motor adaptation were substantially slowed down by decreasing calcium levels from 2.8 mM to 0.05 mM (Ricci *et al*. 2003). Adequately the changes in frequency and amplitude of hair-cell bundle oscillations in the bullfrog sacculus exhibit the property that raising calcium concentration raised the frequency and reduced the amplitude, while lowering calcium exhibits the reverse effect.

The seminal paper by Lumpkin and Hudspeth (1998) presented the experimental assay about regulation of free Ca^{2+} ions in hair-cell stereocilia. The authors used confocal microscopy to detect Ca^{2+} ions entry and distribution within stereocilia of hair cells. They also developed a model of stereociliary Ca^{2+} homeostasis with appropriate regulatory mechanisms. Their theoretical approach is very complex, being described by a system of seven differential equations. They claimed that 'although images were collected from hundreds of stereocilia most were not suitable for fitting with that model'. In the other publication by the same authors (Lumpkin and Hudspeth 1995), it was realized that regulatory mechanism of Ca^{2+} fluxes must be located in stereocilia shaft region which is densely packed with bundled actin filaments. Otherwise in an exhaustive review article, Gartzke and Lange (2002) have stressed that the bundles of microfilaments are forming a diffusion barrier so that the polyelectrolyte nature of actin filaments plays a crucial role in Ca^{2+} signaling in stereocilia.

Interestingly in despite of the fact that Ca^{2+} ions play leading role in controlling the active force generation by Myo1c motors, the concentration of these ions is marginally small compared with that of dominant K^+ ions. The very seminal experimental assay by Beurg *et al*. (2010) performed in rat hair cells revealed that when the influx current through hair bundle channels amounts 3.4 nA, just 0.2% ot this current is carried by Ca^{2+} ions with corresponding peak current of the order of 7 pA. And more than that; little is known about the equilibria between ionized and nonionized calcium fraction in the hair cell's endolymph. Some evidences show that the total calcium concentration is by one order of magnitude higher than the ionized fraction. It opens the question of how this low concentration of Ca^{2+} ions can be properly distributed in order to be on right time at the right places to provide so concerted cell's responses to complex auditory signals.

All these facts motivated us to elaborate a new approach in order to try to explain still uncompleted answer of how calcium mediates so efficiently this active nonlinear mechanism of auditory sensitivity. The approach is strongly relied on the fact that actin filaments within the hair bundles exhibit polyelectrolyte properties in natural endolymph. So the effect of counterion condensation (Manning 1978) could be safely expected to take place for these cytoskeletal filaments. The additional arguments were found in the circumstance that earlier experimental evidences (Lin and Cantiello 1993; Priel *et al*. 2006) and some theoretical contributions (Tuszynski *et al*. 2004; Sataric *et al*. 2009a, b; Sekulic *et al*. 2011) suggested that both microtubules and actin filaments, as being polyelectrolytes in physiological conditions, significantly increase ionic currents even exhibiting conspicuous effects of current amplification.

The paper is organized as follows: In section 2, we explained the polyelectrolyte character of actin filaments and quote some earlier models. In section 3, we applied the standard Manning's model (Manning 1996, 2011) for the condensation of calcium ions on the actin filaments within the stereocilia. Using the trawling-wave approach, the problem is solved exactly. Section 4 provides discussion and conclusions.

2. Actin filaments as polyelectrolytes

It is well known that first conspicuous biological example of typical polyelectrolyte was DNA under physiological conditions. This circumstance has very essential impact on the functional properties of these sophisticated molecules. The phenomenon of DNA condensation has been successfully elaborated by the theory of linear polyelectrolytes (Manning 1978, 1993, 2008). A double stranded DNA at neutral pH has a linear charge spacing b = 0.17 nm, much less than the Bjerrum length.

The Bjerrum length l_B defines the distance at which the thermal fluctuations are equal to the electrostatic attraction or repulsion between ions in solution whose relative dielectric constant is ε. For univalent ions and for a given absolute temperature T it reads (Israelachvili 1992):

$$\frac{e^2}{4\pi\varepsilon_r\varepsilon_0 l_B} = k_B T \quad \Rightarrow \quad l_B = \frac{e^2}{4\pi\varepsilon_r\varepsilon_0 k_B T}, \tag{1}$$

where $e = 1.6\times10^{-19}$ C is the elementary charge, $\varepsilon_0 = 8.85\times10^{-12}$ F/m is the permittivity of the vacuum and k_B =

1.38×10^{-23} J/K is Boltzmann's constant. It follows that for $T = 310$ K and $\varepsilon_r = 80$ this parameter has the value

$$l_B = 0.67\,\text{nm}. \tag{2}$$

Actin filaments are abundant cytoskeletal structures that play the important roles in a variety of cell functions including locomotion, cell shape and auditory processes. The globular actin monomers of diameter $d = 5.4$ nm polymerize to double stranded filaments form, so called F-actin, see figure 3. The polyelectrolyte nature of actin filaments was noticed some twenty years ago (Lin and Cantiello 1993), and the adequate values of relevant parameters were estimated (Tang and Janmey 1996). The already mentioned review by Gartzke and Lange (2002) considers different theoretical and experimental concepts of actin filaments as typical polyelectrolytes in providing the signaling pathways for Ca^{2+} ions. Our approach is in accord with this strategy but has originality and plausibility. Each monomer carries an excess of 14 negative charges, three of which are neutralized by protonation of three pertaining histidines per monomer at pH = 7.2. It provides that remaining 11 charges give the linear charge density of approximately 4 *e*/nm. This fact has the fundamental implication that the linear charge spacing along the filament axis b=0.25 nm is sufficiently small compared to the Bjerrum length to make the counterion condensation theory relevant. The corresponding dimensionless parameter ξ for the univalent ions is greater than unity

$$\xi = \frac{l_B}{b} = 2.7 > 1. \tag{3}$$

In our approach related for the stereocilia, we contemplated that pertaining actin filaments should be surrounded primarily by divalent Ca^{2+} ions forming screened 'condensed cloud'. In that shielded layer one could estimate the corresponding local Bjerrum length to be twice greater than in the univalent case, equation (2), since the charge is $z = 2$, giving:

$$l_B = 1.34\,\text{nm}. \tag{4}$$

Accordingly, the parameter that indicates the polyelectrolyte nature of actin filament now reads:

$$\xi = 5.4. \tag{5}$$

Around this 'condensed cloud' there is the layer of thickness equal to Bjerrum length and which is depleted of ions of both signs. This argument brings about that one could consider an actin filament as a capacitor capable to store and transport localized Ca^{2+} counterions along its length (Sataric *et al*. 2009a). The other important parameter relevant for polyelectrolytes is Debye screening length Δ, defined in a way to depend on total ionic concentration in a given solution. For typical hair cell's endolymph (Israelachvili 1992), the average ionic number concentration is of the order of $c_s = 150$ mol/m^3. Taking $N_A = 6\times10^{23}$ 1/mol, we easily get:

$$n_s = N_A c_s = 9 \times 10^{25}\,1/\text{m}^3. \tag{6}$$

In as much the Debye length is defined as

$$\Delta = \left(\frac{\varepsilon_r \varepsilon_0 k_B T}{2e^2 n_s}\right)^{1/2}, \tag{7}$$

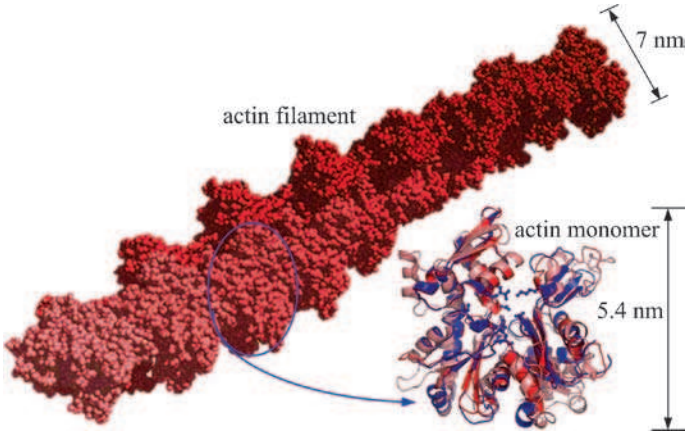

Figure 3. Structure model of actin filament consisting of two intertwined long-pitch right-handed helices is shown on the left. Actin monomer ribbon structure is shown on the right.

using the same set of parameter as in equation (1) along with equation (6), one easily gets

$$\Delta = 0.81 \times 10^{-9}\,\mathrm{m}. \tag{8}$$

We are now able to start from the Manning's polyelectrolyte theory (Manning 2011), introducing electrolytic free energy G of an actin filament with N condensed counterions (in the case of stereocilia the Ca^{2+} ions) and defining the dimensionless density of free energy g:

$$g = \frac{G}{Nk_{\mathrm{B}}T} = -(1-z\theta)^2\xi\ln\left(\frac{\mathrm{b}}{\Delta}\right) + \theta\ln\left(\frac{\theta}{Q}\right). \tag{9}$$

The first term in this expression arises from the sum of Debye-screened repulsions between all pairs of negative sites on the charged filament. Since $\mathrm{b}/\Delta = 0.313$ and $\ln(\mathrm{b}/\Delta) = -1.163$, the first term in equation (9) is positive as required. The quantity θ is the number of Ca^{2+} counterions condensed on the charged actin filament per single charge site (negative). This is the fraction less than unity at low ionic concentration. The parameter b is introduced earlier, but its inverse value $\mathrm{b}^{-1} = 4\times10^{9}$ m^{-1} is the number of negative sites on the filament per unit length, bringing about that the linear concentration of condensed counterions obeys the inequality

$$\frac{\theta}{\mathrm{b}} \le \frac{1}{\mathrm{b}}. \tag{10}$$

From this reason the effective charge of a site is reduced from a former bare unit charge 1 to the following fraction for Ca^{2+} counterions

$$1-z\theta = 1-2\theta. \tag{11}$$

The second term in equation (9) is of ideal-gas type free energy, where Q stands for an internal partition function which contains the short-range interactions between the condensed calcium counterions and actin filament but is assumed to be independent of θ.

The expression given by equation (9) enables us to calculate the electrochemical potential of the condensed counterions as follows:

$$\mu_c = k_{\mathrm{B}}T\frac{\partial g}{\partial\theta} = 2k_{\mathrm{B}}Tz(1-z\theta)\xi\ln\left(\frac{\mathrm{b}}{\Delta}\right) + k_{\mathrm{B}}T\left[\ln\left(\frac{\theta}{Q}\right)+1\right]. \tag{12}$$

If the filament with counterions is subjected to the constant external electric field E, parallel to filament axis x, the corresponding potential energy is

$$E_{\mathrm{p}} = -zeEx. \tag{13}$$

The equilibrium state of counterions on an actin filament can be inferred if above chemical potential μ_{c} is compared with the chemical potential of the free counterions, which at low ionic concentration c_{s} equals

$$\mu_{\mathrm{free}} = 2k_{\mathrm{B}}T\ln(c_{\mathrm{s}}). \tag{14}$$

For already used concentration c_{s} = 150 mol/m^3 for endolymph, we can compare logarithmic factors

$$\ln\left(\frac{\mathrm{b}}{\Delta}\right) \cong \ln(c_{\mathrm{s}}), \tag{15}$$

and it is apparent that equality of both chemical potential, Eqs. (12) and (14), is provided for a discrete positive fractional value θ_0, if the following condition holds:

$$z(1-z\theta_0)\xi = 1; \quad \theta_0 = \frac{1}{z}\left(1-\frac{1}{z\xi}\right). \tag{16}$$

The fractional coverage of bare negative sites along an actin filament θ_0 is the equilibrium value that is constant along the length of the filament in the absence of an applied electric field or equivalently without the influx of Ca^{2+} ions from transduction channels. Substituting in equation (16) the valence of Ca^{2+} ions $z = 2$ and $\xi = 5.4$, we get

$$\theta_0 = 0.45, \tag{17}$$

while for monovalent counterions with $\xi = 2.7$ one obtains $\theta_0 = 0.4$. The fraction of remaining negatively charged sites on an actin filament is adequately expressed as:

$$1-z\theta_0 = 0.1. \tag{18}$$

In the following section, we will use the above approach to analyze the dynamics of calcium ions along actin filaments in the context of hair bundle active adaptation within an auditory process. Shortly we should mention here that some earlier attempts were made in order to clarify the experimental results (Lin and Cantiello 1993) exhibiting the enhanced ionic currents along actin filaments *in vitro*. These models (Tuszynski *et al*. 2004; Sataric *et al*. 2009a) were based on the assumption that actin filaments possess the features of nonlinear electric transmission lines and also by taking into account the polyelectrolyte character of actin filaments. Sequencing a filament into series of elementary units represented by actin monomers and considering them as small capacitors and resistors, we earlier estimated (Sataric *et al*. 2009a) the elementary capacitance to be of the order of $C_0 \sim 10^{-16}$ F and respective ohmic

resistance $R_0 \sim 10^8\ \Omega$. The corresponding characteristic time of discharging such elementary unit is thus given as

$$T_0 = R_0 C_0 \approx 10^{-8}\ \mathrm{s}. \tag{19}$$

Since the length of this elementary unit is the diameter of an actin monomer $d = 5.4$ nm, the velocity of migration of ionic waves along a filament is of the order of a few decimeters per second. This is much more reasonable result compared with very high velocity estimated by Tuszynski *et al*. (2004), which is physically intractable.

3. The nonlinear flux equation for the propagation of Ca^{2+} ions along actin filaments

Let us concentrate on the analysis of how the influx of Ca^{2+} ions through transduction channels can be distributed along actin filaments within the stereocilia. Every single influx is accompanied by the gradient of voltage and the presence of consecutive field E which may depend on time. It brings about that the concentration of the condensed counterions becomes a function both of the time and of the coordinate x directed along the pertinent actin filament. Then the linear concentration of condensed counterions must obey the continuity condition

$$\frac{1}{\mathrm{b}}\frac{\partial \theta}{\partial t} = -\frac{\partial J}{\partial x}, \tag{20}$$

where $J(x,t)$ stands for the Ca^{2+} flux confined along a filament and being the product of linear concentration of Ca^{2+} ions θ/b and their average drift velocity v_d. The drift velocity is provided with the force F acting on an ion and being balanced by the friction of viscosity characterized by the parameter λ

$$F = \lambda v_\mathrm{d}; \quad v_\mathrm{d} = \frac{F}{\lambda}. \tag{21}$$

Thus the ionic flux is expressed as

$$J(x,t) = \frac{\theta}{\mathrm{b}}\left(\frac{F}{\lambda}\right). \tag{22}$$

The force F is primarily the consequence of the presence of the negative gradient of electrochemical potential, given by equation (12), with addition of electric field, Eq (13)

$$F = -\frac{\partial}{\partial x}(\mu_\mathrm{c} - zeEx). \tag{23}$$

In that respect the flux equation (22) becomes

$$J(x,t) = \frac{ze}{\mathrm{b}\lambda}E\theta - \frac{k_\mathrm{B}T}{\lambda}\left[1 - 2z^2\xi\theta\ln\left(\frac{\mathrm{b}}{\Delta}\right)\right]\frac{\partial \theta}{\partial x}, \tag{24}$$

and this implies that on the basis of continuity condition, Eq (20), the equation of motion for concentration of counterions $\theta(x,t)$ has the following shape:

$$\frac{\partial \theta}{\partial t} = -\frac{ze}{\lambda}E\frac{\partial \theta}{\partial x} + \frac{k_\mathrm{B}T}{\lambda}\frac{\partial^2 \theta}{\partial x^2} - \frac{k_\mathrm{B}T}{\lambda}2z^2\xi\ln\left(\frac{\mathrm{b}}{\Delta}\right)\left(\frac{\partial \theta}{\partial x}\right)^2 - \frac{k_\mathrm{B}T}{\lambda}2z^2\xi\ln\left(\frac{\mathrm{b}}{\Delta}\right)\left(\theta\frac{\partial^2 \theta}{\partial x^2}\right). \tag{25}$$

This is obviously the nonlinear partial differential equation of second order. In the case of the presence of the field of small amplitude, Manning (2011) used to linearize the above master equation by neglecting the nonlinear term of gradient squared and also replaced θ in front of second derivative by the equilibrium value θ_0, given by equation (16). It reduced the nonlinear equation to standard diffusion equation. We will return to this option later. Now we will solve equation (25) exactly by the specific procedure applied for solitonic waves. This was motivated by the fact that equation (25) contains the dispersive term $\left(\frac{\partial^2 \theta}{\partial x^2}\right)$ which competes with two nonlinear terms present here.

First, we assume that the influx of Ca^{2+} ions creates the nonequilibrium concentration $\theta(x,t) > \theta_0$, which flows along actin filament in the traveling wave form

$$\theta(x,t) = \theta\left(\frac{x}{l_0} - v\frac{t}{l_0}\right), \tag{26}$$

where $l_0 = 5.4$ nm stands for the length of an actin monomer and v is wave velocity. We should go over to the dimensionless coordinate ζ and time τ with the velocity s, as follows:

$$\zeta = \frac{x}{l_0}; \quad \tau = \frac{t}{T_0}; \quad s = \frac{v}{v_0}; \quad \mathrm{v}_0 = \frac{l_0}{T_0}. \tag{27}$$

The characteristic cut-off velocity v_0 is defined by the time T_0 for what the drift of counterions passes by a single monomer of the length l_0. Therefore expression (26) now reads

$$\theta = \theta(\zeta - s\tau) = \theta(\varphi); \quad \varphi = \zeta - s\tau. \tag{28}$$

On the basis of Eqs. (26) and (28), we have the set of transformations:

$$\frac{\partial\theta}{\partial t}=\frac{\partial\theta}{\partial\tau}\frac{\partial\tau}{\partial t}=\frac{1}{T_0}\frac{\partial\theta}{\partial\tau};\quad \frac{\partial\theta}{\partial x}=\frac{\partial\theta}{\partial\zeta}\frac{\partial\zeta}{\partial x}=\frac{1}{l_0}\frac{\partial\theta}{\partial\zeta};$$
$$\frac{\partial\theta}{\partial\tau}=-s\frac{d\theta}{d\varphi};\frac{\partial\theta}{\partial\zeta}=\frac{d\theta}{d\varphi}. \tag{29}$$

Eventually by taking all exposed transformations given by equation (29) and inserting them in equation (25), instead of partial differential equation, problem is reduced to a nonlinear ordinary differential equation as follows:

$$-\frac{s}{T_0}\frac{d\theta}{d\varphi}=-\frac{ze}{\lambda}\frac{E}{l_0}\frac{d\theta}{d\varphi}+\frac{k_BT}{\lambda l_0^2}\frac{d^2\theta}{d\varphi^2}-\frac{k_BT}{\lambda l_0^2}$$
$$2z^2\xi\ln\left(\frac{b}{\Delta}\right)\left(\frac{d\theta}{d\varphi}\right)^2-\frac{k_BT}{\lambda l_0^2}2z^2\xi\ln\left(\frac{b}{\Delta}\right)\left(\theta\frac{d^2\theta}{\partial\varphi^2}\right). \tag{30}$$

After simple rearrangement this equation can be brought into this compact form:

$$\alpha\frac{d\theta}{d\varphi}+(\beta+\theta)\frac{d^2\theta}{d\varphi^2}+\left(\frac{d\theta}{d\varphi}\right)^2=0, \tag{31}$$

where the two abbreviations were introduced:

$$\alpha=\left(s\frac{l_0^2}{T_0}-\frac{zel_0E}{\lambda}\right)\left[-\frac{k_BT}{\lambda}2z^2\xi\ln\left(\frac{b}{\Delta}\right)\right]^{-1};$$
$$\beta=\left[-2z^2\xi\ln\left(\frac{b}{\Delta}\right)\right]^{-1}. \tag{32}$$

We could reduce the order of equation (31) by the substitutions:

$$\frac{d\theta}{d\varphi}=y(\theta);\quad \frac{d^2\theta}{d\varphi^2}=yy', \tag{33}$$

thus getting the linear differential equation of first order :

$$y'+\frac{1}{\beta+\theta}y=-\frac{\alpha}{\beta+\theta}. \tag{34}$$

After a straightforward calculation and finding the constants of integration from the following conditions

$$\left.\begin{array}{l}\text{for}\quad \theta=\theta_0;\quad y=0,\\ \text{for}\quad \varphi=0;\quad \theta=\theta_0,\end{array}\right\} \tag{35}$$

we obtain the solution in the form of an implicit function $\theta(\varphi)$

$$\theta-\theta_0+(\theta_0-\beta)\ln(\theta-\theta_0)=-\frac{\alpha\beta}{\beta+\theta_0}\varphi. \tag{36}$$

If we introduce the new variable

$$\Delta\theta=\theta-\theta_0=w, \tag{37}$$

the above equation reduces to the simpler version

$$w+(\theta_0-\beta)\ln w=-\frac{\alpha\beta}{\beta+\theta_0}\varphi. \tag{38}$$

Now is the moment to estimate parameters α and β in order to prepare final equation for numerical treatment. It is very easy to calculate β on the basis of definition, see equation (32). Inserting z = 2, ξ = 5.4 and ln(b /Δ) = -1.163, the estimated value of β is

$$\beta=0.02;\quad \beta<<\theta_0=0.45. \tag{39}$$

In the other hand, looking for the parameter α we need to know the viscosity factor λ for a single ion, the order of magnitude of electric field, and the ratio l_0^2/T_0 which has the dimension of the constant of diffusion. The dimensionless wave velocity s could be taken to be exactly one. So, the estimation of parameter α has more uncertainty. Nevertheless we will do it as follows. The viscosity acting on a single Ca^{2+} ion can be roughly estimated for the bulk solution first, starting from Stokes' law of viscous force acting on the sphere

$$F=6\pi\eta rv;\quad \lambda=6\pi\eta r. \tag{40}$$

If the viscosity constant is taken for the water it amounts $\eta \sim 10^{-3}$ Pa·s, while the effective radius of Ca^{2+} ions is $r=2\times10^{-10}$ m. It gives the bulk viscosity:

$$\lambda_b\approx3.7\times10^{-12}\,\frac{\text{Ns}}{\text{m}}. \tag{41}$$

But, this bulk viscosity parameter should be multiplied properly. The increased value is the consequence of the fact that the condensed Ca^{2+} counterions reside quite literally on the surface of filament's landscape which is not smooth. We chose arbitrary to multiple it by five yielding

$$\lambda \approx 1.85 \times 10^{-11} \frac{\mathrm{Ns}}{\mathrm{m}}. \tag{42}$$

Dhont and Kang (2010) mentioned that this parameter was taken to be twenty times greater than the bulk value in order to fit their theoretical model with experimental data collected from fd virus. The ratio l_0^2/T_0 can be evaluated on the basis of a few different approaches. First, we can rely on the characteristic time T_0 from equation (19), thus getting

$$\frac{l_0^2}{T_0} \approx \frac{\left(5.4 \times 10^{-9}\right)^2}{10^{-8}} = 2.9 \times 10^{-9} \frac{\mathrm{m}^2}{\mathrm{s}}. \tag{43}$$

The alternative is to use the expression for the diffusion parameter of bulk solution (Dhont and Kang 2011), $D_0 = 2\times10^{-9}$ m^2/s. Third option is the most realistic one and it represents the effective diffusion parameter elaborated by Manning (2011) for linearized version of master equation (25), and expressed as

$$D_{\mathrm{eff}} = \frac{k_B T}{\lambda}\left[1 - 2z^2 \xi \theta_0 \ln\left(\frac{\mathrm{b}}{\Delta}\right)\right], \tag{44}$$

this brings about the numerical value pertinent to Ca^{2+} ions flowing along actin filaments at physiological temperature, yielding:

$$D_{\mathrm{eff}} = 5.4 \times 10^{-9} \frac{\mathrm{m}^2}{\mathrm{s}}. \tag{45}$$

This value is expected to be the best choice because it catches the remarkable features of actin filament as a polyelectrolyte. Very similar results for effective diffusion of counterions were elaborated by Dhont and Kang (2010, 2011). Including above evaluations, we see that for realistic values of intrinsic electric field, which arises from ionic influx through transduction channels and is being in range (10^3–10^4) V/m, the inequality

$$s\frac{l_0^2}{T_0} >> \frac{zel_0E}{\lambda} \tag{46}$$

safely holds. But, if the strong local field of the order of 10^6 V/m is present, then the terms in equation (46) are mutually competitive.

Taking $sl_0^2/T_0 = 6.12\times10^{-9}\mathrm{m}^2/\mathrm{s}$ and $\left[-\frac{k_B T}{\lambda} 2z^2 \xi \ln\left(\frac{\mathrm{b}}{\Delta}\right)\right] = 5.7 \times 10^{-9}\mathrm{m}^2/\mathrm{s}$, we eventually get the parameter α posed in front of first derivative in equation (31)

$$\alpha = 1.07 \tag{47}$$

This enables us to complete the specific numerical expression of equation (38) as follows:

$$w + 0.43 \ln w = -0.046\varphi. \tag{48}$$

The graphical shape of above implicite function representing the ionic pulse is shown in figure 4(A). If we take that wave progresses ten times slower ($s = 0.1$)

$$w + 0.43 \ln w = -0.0046\varphi, \tag{49}$$

it leads to the pulse more spread out along filament as shown in figure 4(B). The symbolic view of charge distribution of Ca^{2+} counterions within the localized pulse is given in figure 5.

This nonlinear pulse propagates along actin filament and pertaining counterions do not leak out into solution in despite of the fact that the concentration of bulk counterions Ca^{2+} is much less than the local concentration within the pulse. It seems paradoxical, but it appears that the electrostatic interactions within the ionic cloud remarkably augment the ordinary diffusion providing that actin filaments are the true pathways of the least resistance for Ca^{2+} ionic current. It assures that the propagation of ionic cloud should be faster and protected of leaking out into the bulk endolymph, thus preventing to be caught by calcium buffers. When an incoming ionic pulse sweeps along actin filament, it performs the control role regarding activities of Myo1c motors bridged to this filament. Then this pulse comes to the end position by cuticular plate, the cytoskeletal anchor for the stereocilia bundle, where mitochondria are conspicuously concentrated. The mitochondria are primarily responsible for generating adenosine 5'-triphosphate (ATP) that fuels Myo1c motors. Mitochondria also affect Ca^{2+} balance fueling PMCA pumps that extrude calcium from hair bundle and themselves act as a large-capacity calcium store (Nicholls 2005).

Let us now consider shortly of how Ca^{2+} ions influence the cross-bridge cycle of Myo1c motors in hair bundles. It was shown experimentally (Adamek *et al*. 2008) that calcium inhibits the rate of ATP hydrolysis process which powers the energy for Myo1c strength and at the same time calcium accelerates the release of ADP, the product of hydrolysis. In that way calcium induces the accelerations of cross-bridge detachment enabling Myo1c to slide or climb up along actin filament. The transient increase in calcium concentration should reduce the stiffness of the so called lever arm of

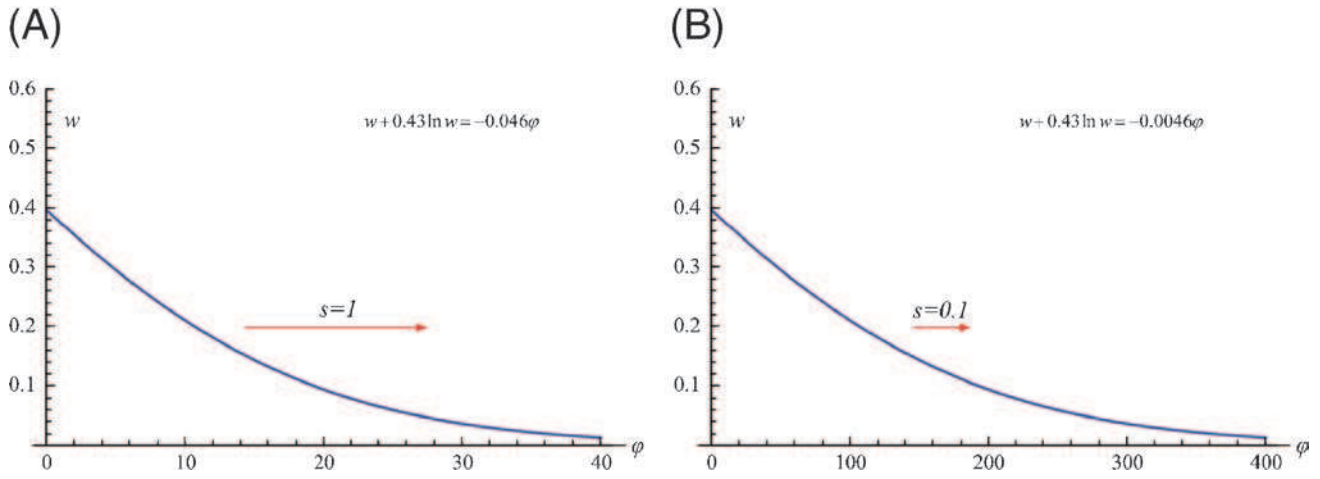

Figure 4. (**A**) Numerical solution of the function $w(\varphi)$ if dimensionless velocity s is equal to 1. (**B**) The shape of the same function for ten time slower pulse (s = 0.1). This pulse is spread out remarkably in comparison with first one.

Myo1c. This is lowering the strain in the same motor allowing ADP to escape and motor itself to detach from filament and to slide along. The detachment of motor is followed by the ATP hydrolysis before the cross-bridge to actin filament is reestablished. In the presence of Ca^{2+} ions, the 7-fold reduction in the rate constant for ATP hydrolysis should adequately increase the life time of detached state, allowing longer time for slippage of a motor along the filament (Adamek *et al*. 2008). It was already stressed that troponin molecules are important mediators in this catalytic action of Ca^{2+} ions (Karkanevatos 2001).

In the context of the model presented here, it is reasonable that faster ionic pulse will spend shorter time in the vicinity of operating motors. During that time the motor is detached and adapts its position in order to remove the cause that brought about its deactivation. If we take that the cut-off velocity of ionic pulse

$$v_0 = \frac{l_0}{T_0} = \frac{5.4 \times 10^{-9}}{10^{-8}} \approx 0.54 \frac{\mathrm{m}}{\mathrm{s}}, \tag{49}$$

and the length of that pulse from figure 4(A) is $\Delta L = 20 \times l_0 \approx 0.11\mu\mathrm{m}$, the corresponding time of Ca^{2+} impact on Myo1c is of the order of

$$\tau = \frac{\Delta L}{v_0} = \frac{0.11\mu\mathrm{m}}{0.54 \frac{\mathrm{m}}{\mathrm{s}}} \approx 0.21 \times 10^{-6}\mathrm{s}. \tag{50}$$

For the case represented in graph from figure 4(B), the time is longer for two orders of magnitude $\tau \approx 2.1 \times 10^{-5}$ s. Generally, the pulses with lower velocity should spend more time in catalyzing the detachment of motors and they tune the processes of lower frequencies. The velocity and the length of a pulse are determined by the opening dynamics of transduction channels, which in turn is dictated by the incoming acoustic signals.

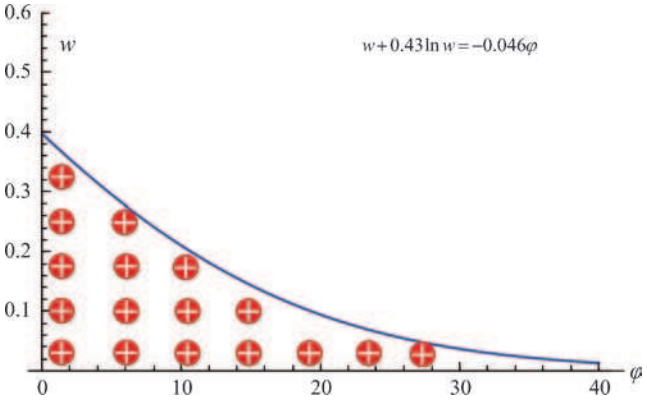

Figure 5. The symbolic view of charge distribution of Ca^{2+} counterions within localized pulse.

4. Discussion and conclusion

At least two motives were the reason for us in an attempt to contribute in resolving the very important problem of how calcium ions efficiently control the activities of Myo1c adaptation motors, implicated in mechanoelectrical transduction in the stereocila of the inner ear. First one is the fact that actin filaments are the true polyelectrolytes *in vivo* conditions and the very profound theory of rodlike polyelectrolytes was systematically developed by Manning (1978, 1993, 1996, 2011). Secondly, we were intrigued by some earlier experiments (Lin

and Cantiello 1993; Priel *et al*. 2006) which indicated that actin filaments and microtubules exhibit the amplifying effect for ionic conduction in dilute solution, *in vitro*.

In the introduction we shortly explained the mechanisms of mechanoelectrical transduction of hair cells emphasizing the role of Ca^{2+} ions in tuning these mechanisms. The polyelectrolytes nature of actin filaments was carefully documented with estimations of relevant parameters as linear charge spacing, the Bjerrum length, Debye length and fractional coverage of a filament with calcium counterions. In parallel, we made a short reminder of our earlier approach based on the electric transmission line model for ionic flow along actin filaments (Sataric *et al*. 2009a).

The main part of paper is dedicated to the application of seminal Manning's model (Manning 2011) for calcium ionic pulse propagation along actin filaments within the stereocilia. Instead of simplifying the master equation (25), we performed an exact solution using the unified space-time variable φ for traveling wave. That was initiated by the fact that nonlinear character of equation (25) suggests that the competition between dispersion, governed by the second derivative term, and nonlinearity, represented by the gradient squared term, should lead to creation of a kind of stable pulse localized enough to persist propagating with gradual distortion due to the friction. Second argument for such expectation was the one-dimensionality of this phenomenon which prevents the spatial dispersion. We obtained the solution which is somewhere between kink-like and usual diffusive profile, and which propagates with roughly estimated velocities bounded with cut off value of the order of decimetres per second. Based on such estimations, we were able to extract the conclusion that this mechanism of calcium distribution within stereocilia must be much more efficient than ordinary bulk diffusion. These shielded pulses of ionic clouds are more suitable to fast reach the Myo1c motors and to control their activities. The general outcome is that Ca^{2+} ions within a pulse accelerate of cross-bridge detachment and increase lifetime of detached cross-bridge. The time scale of this process is dictated by the velocity and the length of a single pulse which is defined by the time course of opening and closing of pertinent ionic channels.

Beurg *et al*. (2010) found that raising the calcium level close to hair-cell transduction channels increases the oscillating frequency of hair bundle and decreases its amplitude. Since increased Ca^{2+} level enables injection of faster pulse along actin filament, this pulse detaches for shortly Myo1c motors and they catch the filament soon again reversing the direction of movement of the bundle. In a word, these short and fast pulses accelerate cross-bridge attachment-detachment dynamics. The opposite is true for slow pulses dictated by small influx through transduction channels.

The quantitative relation of ionic pulses with mechanoelastic performances of hair bundles will be presented in a separated article. In final conclusion, it is very probably that Ca^{2+} ions play similar roles in insulin-mediated glucose uptake in which Myo1c is also basically implicated (Bose *et al*. 2002).

Acknowledgements

This research was supported by the Ministry of Education, Science and Technological Development of the Republic of Serbia through Projects: OI171009 and III43008, and Project of Serbian Academy of Sciences and Arts.

References

Adamek N, Coluccio LM and Geeves MA 2008 Calcium sensitivity of the cross-bridge cycle of Myo1c, the adaptation motor in the inner ear. *Proc. Natl. Acad. Sci. USA* **105** 5710–5715

Beurg M, Nam JH, Chen Q and Fettiplace R 2010 Calcium balance and mechanotransduction in rat cochlear hair cells. *J. Neurophysiol.* **104** 18–34

Bose A, Guilherme A, Robida SI, Nicoloro SMC, Zhou QL, Jiang ZY, Pomerleau DP and Czech MP 2002 Glucose transporter recycling in response to insulin is facilitated by myosin Myo1c. *Nature* **420** 821–824

Dhont JKG and Kang K 2010 Electric-field-induced polarization and interactions of uncharged colloids in salt solutions. *Eur. Phys. J. E.* **33** 51–68

Dhont JKG and Kang K 2011 Electric-field-induced polarization of the layer of condensed ions on cylindrical colloids. *Eur. Phys. J. E.* **34** 40

Gartzke J and Lange K 2002 Cellular target of weak magnetic fields: ionic conduction along actin filaments of microvilli. *Am. J. Physiol. Cell Physiol.* **283** C1333–C1346

Gillespie PG and Cyr JL 2004 Myosin-1c, the hair cell's adaptation motor. *Annu. Rev. Physiol.* **66** 521–549

Helmholtz HLF 1954 *On the sensations of tone as a physiological basis for theory of music* (New York: Dover Publications)

Israelachvili JN 1992 *Intermolecular and surface forces: With applications to colloidal and biological systems* (London: Academic Press)

Karkanevatos A 2001 Ultrastructural localization of cytoskeletal proteins in guinea-pig cochlear hair cells. M. Phil Thesis, Keele University, UK

Lin EC and Cantiello HF 1993 A novel method to study the electrodynamic behavior of actin filaments. Evidence for cable-like properties of actin. *Biophys. J.* **65** 1371–1378

Lumpkin EA and Hudspeth AJ 1995 Detection of Ca^{2+} entry through mechanosensitive channels localizes the site of mechanoelectrical transduction in hair cells. *Proc. Natl. Acad. Sci. USA* **92** 10297–10301

Lumpkin EA and Hudspeth AJ 1998 Regulation of free Ca^{2+} concentration in hair-cell stereocilia. *J. Neurosci.* **18** 6300–6318

Manning GS 1978 The molecular theory of polyelectrolyte solutions with applications to the electrostatic properties of polynucleotides. *Q. Rev. Biophys.* **11** 179–246

Manning GS 1993 A condensed counterion theory for polarization of polyelectrolyte solutions in high fields. *J. Chem. Phys.* **99** 477–486

Manning GS 1996 Counterion condensation theory constructed from different models. *Phys. A.* **231** 236–253

Manning GS 2008 Approximate solutions to some problems in polyelectrolyte theory involving nonuniform charge distributions. *Macromolecules.* **41** 6217–6227

Manning GS 2011 A counterion condensation theory for the relaxation, rise, and frequency dependence of the parallel polarization of rodlike polyelectrolytes. *Eur. Phys. J. E.* **34** 39

Martin P, Bozovic D, Choe Y and Hudspeth AJ 2003 Spontaneous oscillation by hair bundles of the bullfrog's sacculus. *J. Neurosci.* **23** 4533–4548

Nam JH, Cotton JR, Peterson EH and Grant W 2006 Mechanical properties and consequences of stereocilia and extracellular links in vestibular hair bundles. *Biophys. J.* **90** 2786–2795

Nicholls DG 2005 Mitochondria and calcium signaling. *Cell Calcium.* **38** 311–317

Priel A, Ramos AJ, Tuszynski JA and Cantiello HF 2006 A biopolymer transistor: electrical amplification by microtubules. *Biophys. J.* **90** 4639–4643

Ricci AJ, Crowford AC and Fettiplace R 2003 Tonotopic variation in the conductance of the hair cell mechanotransducer channel. *Neuron* **40** 983–990

Ruggero MA 1992 Responses to sound of the basilar membrane of the mammalian cochlea. *Curr. Opin. Neurobiol.* **2** 449–456

Sataric MV, Bednar N, Sataric BM and Stojanovic G 2009a Actin filaments as nonlinear RLC transmission lines. *Int. J. Mod. Phys. B.* **23** 4697–4711

Sataric MV, Ilic DI, Ralevic N and Tuszynski JA 2009b A nonlinear model of ionic wave propagation along microtubules. *Eur. Biophys. J.* **38** 637–647

Sekulic DL, Sataic BM, Tuszynski JA and Sataric MV 2011 Nonlinear ionic pulses along microtubules. *Eur. Phys. J. E.* **34** 49

Tang JX and Janmey PA 1996 The polyelectrolyte nature of F-actin and the mechanism of actin bundle formation. *J. Biol. Chem.* **271** 8556–8563

Tuszynski JA, Portet S, Dixon JM, Luxford C and Cantiello HF 2004 Ionic wave propagation along actin filaments. *Biophys. J.* **86** 1890–1903

MS received 14 October 2014; accepted 23 July 2015

Corresponding editor: Vidita A Vaidya